

# Dynamical characteristics of solitary waves, shocks and envelope modes in kappa-distributed non-thermal plasmas: an overview

I. Kourakis<sup>1</sup>, S. Sultana<sup>1</sup> and M. A. Hellberg<sup>2</sup>

<sup>1</sup>Centre for Plasma Physics, Department of Physics and Astronomy, Queen's University Belfast, BT7 1NN Northern Ireland, UK

<sup>2</sup>School of Chemistry and Physics, University of KwaZulu-Natal, Private Bag X54001, Durban 4000, South Africa

E-mail: IoannisKourakisSci@gmail.com

**Abstract.** Space plasmas provide abundant evidence of highly energetic particle population, resulting in a long-tailed non-Maxwellian distribution. Furthermore, the first stages in the evolution of plasmas produced during laser-matter interaction are dominated by nonthermal electrons, as confirmed by experimental observation and computer simulations. This phenomenon is efficiently modelled via a kappa-type distribution. We present an overview, from first principles, of the effect of superthermality on the characteristics of **electrostatic plasma waves**. We rely on a fluid model for **ion-acoustic** excitations, employing a kappa distribution function to model excess superthermality of the electron distribution. Focusing on nonlinear excitations (solitons), in the form of solitary waves (pulses), shocks and envelope solitons, and employing standard methodological tools of nonlinear plasmadynamical analysis, we discuss the role of excess superthermality in their propagation dynamics (existence laws, stability profile), geometric characteristics and stability. Numerical simulations are employed to confirm theoretical predictions, namely in terms of the stability of electrostatic pulses, as well as the modulational stability profile of bright- and dark-type envelope solitons.

## 1. Introduction

Space plasma observations provide abundant evidence for the existence of highly energetic particles (electrons, in principle) at velocities exceeding the thermal speed [1, 2]. The presence of this *excess superthermal* component, which may be due to various acceleration mechanisms, gives rise to a long-tailed velocity distribution which may deviate substantially from the Maxwellian. Aiming at an interpretation of the power-law dependence of the velocity distribution observed in Space environments, a parametrized distribution function was proposed in the 1960s, characterized by a real parameter  $\kappa$  (*kappa*) [1, 3]. The *kappa* distribution function ( $\kappa$ -*df*) was subsequently widely employed in the interpretation of observed spectra, and was often proven to fit data more accurately than the Maxwellian approach [3, 4]. Success stories in this field include the use of a bi-kappa approach in comparison with the standard bi-Maxwellian model in the study of the Saturn magnetosphere [4, 5] and a recent study of dust-particle charging in nonthermal electron environments, with application in electromagnetic

wave propagation in the solar system [6]. In the laboratory, the kappa distribution was recently employed in experimental studies of electron-holes [7]. Generation of a superthermal particle population was also observed in high-power laser plasma interactions, where electron acceleration was induced by plasma expansion [8], associated with the creation of a shock [9]. Excess superthermality thus arises as an ubiquitous paradigm in plasma dynamics.

It has been shown that excess electron superthermality may alter the propagation characteristics of plasma modes, a fact to first approach attributed to the dramatic modification of Debye screening properties [10]. We have recently undertaken a comprehensive series of investigations, from first principles, of the effect of superthermality on the characteristics of plasma modes [11–16, 18]. This is a collective effort, which spans a wide region of plasma modes, ranging from ion-acoustic [11–13] and electron acoustic [14] solitary waves to envelope solitons [15] and shocks [16, 17], complemented by extensive numerical investigations [18]. What follows is a short overview of the relevant framework, complemented by a brief presentation of unpublished recent work.

## 2. Linear wave characteristics in superthermal plasmas

We have earlier proposed a simple model for electrostatic excitations in unmagnetized collisionless nonthermal plasmas [19], consisting of a (“cold”) fluid description for the ion species, **and nonthermal electrons having a  $\kappa$  distribution** [3]

$$f_{\kappa} = \frac{n_{e0}}{(\pi\kappa\theta^2)^{3/2}} \frac{\Gamma(\kappa+1)}{\Gamma(\kappa-1/2)} \left(1 + \frac{v^2}{\kappa\theta^2}\right)^{-(\kappa+1)}. \quad (1)$$

**Here  $n_{e0}$  is the unperturbed (equilibrium) electron density, and the spectral index  $\kappa$  measures the strength of the excess superthermality present in the velocity distribution function. The most probable speed,  $\theta = ([\kappa - 3/2]/\kappa)^{1/2}(2k_B T_e/m_e)^{1/2}$ , is an effective thermal speed, where  $T_e$  is the temperature of the equivalent Maxwellian with the same internal energy. While  $\kappa \rightarrow \infty$  recovers the Maxwellian, small values of  $\kappa > 3/2$  correspond to a strong deviation from the thermal distribution. Integration of  $f_{\kappa}$  over velocity space leads to the electron density [3]  $n_e = n_{e0} \left\{1 - e\phi/[(\kappa - \frac{3}{2})k_B T_e]\right\}^{-\kappa+1/2}$ , which, for  $\kappa \rightarrow \infty$  yields the usual Boltzmann expression,  $n_e = n_{e0} e^{e\phi/k_B T_e}$ , where  $\phi$  is the electrostatic potential. Practically, in fact, Maxwellian-like behaviour is recovered for finite values of  $\kappa$  above  $\simeq 10$ . Normalising the time, space, speed and electrostatic potential variables with respect to the inverse ion plasma frequency  $\omega_{p,i}^{-1} = (m_i/4\pi Z_i^2 n_{i0} e^2)^{1/2}$ , the characteristic (Debye screening) length  $\lambda_{Di} = (k_B T_e/4\pi Z_i n_{i0} e^2)^{1/2}$ , the ion acoustic speed  $c_s = (Z_i k_B T_e/m_i)^{1/2} (= \omega_{p,i} \lambda_{Di})$  and the potential scale  $\phi_0 = k_B T_e/e$ , respectively, one obtains the dispersion relation**

$$\omega^2 = \frac{k^2}{k^2 + C_{\kappa}^2}, \quad (2)$$

where  $\omega$  and  $k$  denote the wave's frequency and wavenumber, scaled by  $\omega_{p,i}$  and  $\lambda_{Di}^{-1}$ , respectively. We have defined  $C_{\kappa}^2 = \frac{\kappa-1/2}{\kappa-3/2}$ . We note that the (Debye) charge screening

mechanism is strongly affected by excess superthermality, leading to a reduced ( $\kappa$ -dependent) **modified screening length** [10]

$$\lambda_{Di}^{(\kappa)} = \left( \frac{\kappa - 3/2}{\kappa - 1/2} \right)^{\frac{1}{2}} \left( \frac{k_B T_e}{4\pi Z_i^2 n_{i0} e^2} \right)^{1/2}. \quad (3)$$

This results in a *modified acoustic speed*: indeed, the *real* sound speed in the plasma becomes  $c_s^{(\kappa)} = \omega_{pi} \lambda_{Di}^{(\kappa)} = c_s^{(\kappa \rightarrow \infty)} \left( \frac{\kappa - 3/2}{\kappa - 1/2} \right)^{1/2}$ , i.e., it is reduced by a numerical factor  $C_\kappa^{-1}$ . The acoustic dispersion relation (2) and the associated group velocity are depicted in Fig. 1.

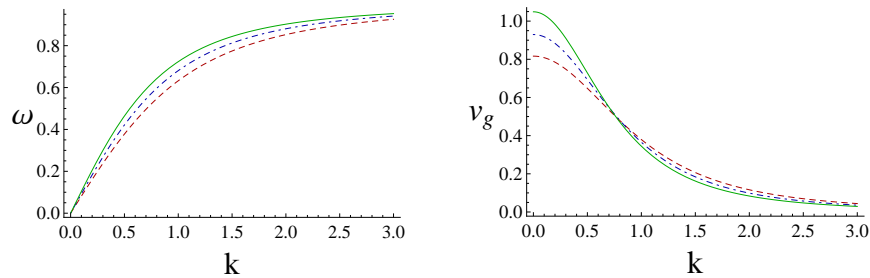


**Figure 1.** (Color online) Dispersion relation: the variation of the ion-acoustic wave frequency  $\omega$  (left panel) and the group velocity  $v_g = d\omega/dk$  (right panel) are depicted versus wavenumber  $k$ , for different values of the superthermality parameter:  $\kappa = 3$  (dashed curves);  $\kappa = 5$  (dot-dashed curves);  $\kappa = 100$  (solid curves) [20].

### 3. Solitary waves

*Large-amplitude nonlinear theory for supersonic pulses.* The existence of large-amplitude ion-acoustic solitary waves was investigated in the past via a pseudopotential method (**known as the “Sagdeev” approach**) [11, 12], a study later extended to dusty plasmas [13]. It was shown that smaller  $\kappa$  values support larger-amplitude electric potential pulses (solitons), associated with stronger bipolar forms for the electric field excitation. Only positive potential pulses occur in electron-ion plasmas. Interestingly, in the presence of charge dust in the plasma, a positive-to-negative soliton polarity shift was predicted for high (negative) dust concentration, prescribing a co-existence of weak negative and large positive pulses, while the associated dust density threshold was shown to be lower for smaller values of  $\kappa$  [13]: superthermality thus favors the existence of negative-potential ion-acoustic pulses. Opposite polarity coexistence was predicted by both Sagdeev and modified-Korteweg de Vries (mKdV) theories, but not by the KdV theory (discussed below). Stationary-profile solitary waves predicted via the pseudopotential method are generally known to occur in specific regions in configuration space, which may be conveniently expressed in terms of the Mach number  $M$ , i.e. the soliton speed scaled by the (reference) sound speed. Generally, the “soliton” existence region is delimited by two values, viz.,  $M_1 < M < M_2$  (e.g.,  $1 < M < 1.58$  in the original Sagdeev [23] ion-acoustic shock model), where  $M_1$  is essentially the true acoustic speed for a given plasma configuration (and depends on the latter and, namely, on the value of the  $\kappa$  parameter) –thus prescribing supersonic soliton propagation– while  $M_2$  corresponds to an infinite compression limit, imposed

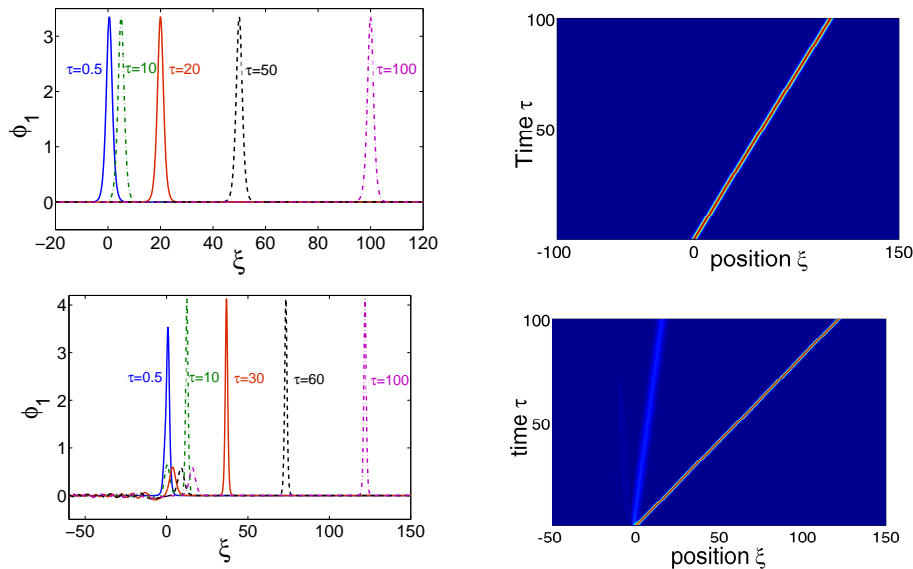


**Figure 2.** (Color online) A high-to-low  $\kappa$  shift is considered. Top panels: Stable propagation of an electrostatic pulse in a Maxwellian plasma. The exact pulse solution (5) was used as initial condition, taking  $\kappa = 100$  in Eq. (4) [20]. Bottom panels: the same initial condition (still for  $\kappa = 100$ ) is considered as input in Eq. (4), but for  $\kappa = 3$  [24].

by reality requirements for the state variables. **It was shown [11, 12] that both  $M_1$  and  $M_2$  decrease** for lower  $\kappa$  (an interested reader is referred to Fig. 1 in [11]: **the existence region** is thus significantly affected by superthermality, and in fact shrinks to *nil* in the limit  $\kappa \rightarrow 3/2$ . It turns out that *slower* electrostatic excitations are supported in the presence of an excess in the superthermal plasma component(s). The existence of permitted values of  $M$  below unity may easily be misinterpreted as subsonic propagation; we emphasize that this is not true: the solitary wave speed always lies *above* the (true,  $\kappa$ -dependent) sound speed, whose (normalised) value itself may be below unity.

*Korteweg - de Vries small-amplitude theory.* Assuming weakly supersonic small-amplitude electrostatic potential pulses, one may consider the stretched (slow) coordinates  $\xi = \epsilon^{1/2}(x - c_s t)$  and  $\tau = \epsilon^{3/2}t$ , where  $\epsilon \ll 1$  is a small real constant and  $c_s = c_s^{(\kappa)}$  is the sound speed defined above, and expand the dependent variables ( $n$ ,  $u$  and  $\phi$ ) near equilibrium as  $\phi \simeq \epsilon\phi_1 + \epsilon^2\phi_2 + \dots$  (along with analogous expressions for  $n$  and  $u$  near 1 and 0, respectively). The leading-order electrostatic potential disturbance is given by the *Korteweg - de Vries* (KdV) equation

$$\frac{d\phi_1}{d\tau} + A\phi_1 \frac{d\phi_1}{d\xi} + B \frac{d^3\phi_1}{d\xi^3} = 0, \quad (4)$$

where  $A = 2(\kappa - 1)/\sqrt{(2\kappa - 3)(2\kappa - 1)}$  and  $B = \frac{1}{2}[(2\kappa - 1)/(2\kappa - 3)]^{-3/2}$  respectively (recovering  $A = 2B = 1$ , as expected, in the known Maxwellian electron limit,  $\kappa \rightarrow \infty$  [22]).

The KdV equation (4) yields the well-known soliton solution

$$\phi_1(\xi, \tau) = \phi_0 \operatorname{sech}^2\left(\frac{\xi - V\tau}{L_0}\right), \quad (5)$$

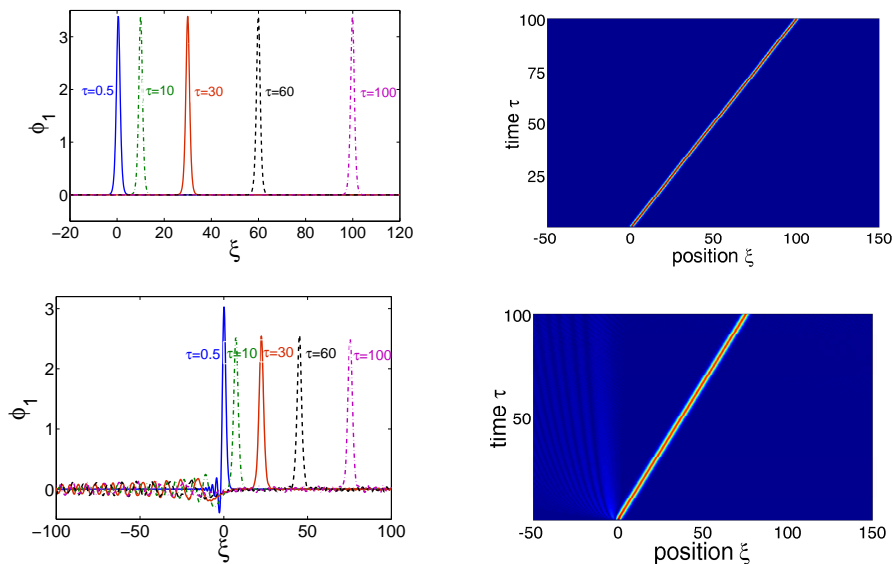


**Figure 3.** (Color online) A low-to-high  $\kappa$  interface is considered. The evolution of a pulse initially moving in a excessively superthermal plasma (for  $\kappa = 3$ , here: top panels) is taken to enter into a Maxwellian region (here  $\kappa = 100$ : bottom panels) at  $t = 0$ . The exact pulse solution (5) was considered as initial condition, for  $\kappa = 3$  into the KdV Eq. (4), evaluated at:  $\kappa = 3$  (top panels) and  $\kappa = 100$  (bottom panels) [24].

where the pulse amplitude  $\phi_0 = 3V/A$  and width  $L_0 = \sqrt{4B/V}$  satisfy  $\phi_0 L_0^2 = 12B/A$ .

We have undertaken a series of numerical simulations, to investigate the dynamical stability profile of KdV solitons in superthermal plasmas (briefly discussed in [19], for dusty plasmas). Adopting, say, the scenario of two colliding plasma clouds, an electrostatic pulse initially propagating in a Maxwellian plasma is assumed to enter a region characterized by a lower value of  $\kappa$ . To this end, we have considered the exact solution Eq. (5) for a high value  $\kappa = 100$ , used as initial condition to integrate Eq. (4), but evaluating the coefficients therein at lower  $\kappa$  ( $= 3$  here: see the lower panels in Fig. 2). The energy stored in the pulse allows it to evolve into a faster (also taller and thinner, as expected) pulse, possibly in addition to a slower (weaker, wider) sister pulse, in the particular case considered in Fig. 2. Pulses crossing into a lower  $\kappa$  region were observed to *accelerate* (to see this, compare the top right to bottom right panels in Fig. 2); this was rather expected, since lower  $\kappa$  values support **faster solitons** [11–13].

Reversing the above scenario, an exact soliton solution of the KdV Eq. (4) evaluated for  $\kappa = 3$ , was assumed to enter a Maxwellian region. The results are depicted in Fig. 3. The pulse slows down slightly and grows wider, while a sea of linear waves are generated behind it, due to the energetic misbalance between the exact soliton solutions for high and for low  $\kappa$ .

We conclude this part by adding that we have recently employed a hybrid KdV-Burgers description to investigate the role of dynamical viscosity, associated with the dynamics of electrostatic *shocks* in kappa-distributed plasmas. The interested reader is referred to [17] for details, which are omitted here.

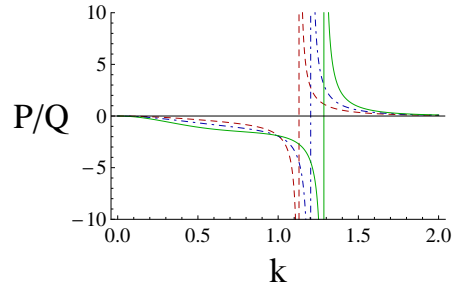


**Figure 4.** (Color online) The ratio  $r = P/Q$  is shown *vs.* the carrier wavenumber  $k$ , for  $\kappa = 3$  (dashed curve);  $\kappa = 5$  (dot-dashed curve);  $\kappa = 100$  (solid curve) [20].

#### 4. Wavepacket stability and superthermal effect

Let us consider the dynamics of an ion-acoustic wavepacket propagating in superthermal plasma. A multiscale approach may be employed [25], based on the fluid model presented above, to separate the fast carrier from the slow envelope wave. The method consists of considering small ( $\epsilon \ll 1$ ) deviations of all state variables, say  $S$  ( $= n, u, \phi$ ) from equilibrium as  $S = S^{(0)} + \sum_{n=1}^{\infty} \epsilon^n \sum_{l=-n}^n S^{(nl)} e^{il(kx - \omega t)}$ , where the  $l$ -th harmonic amplitudes  $S^{(nl)}$  are assumed to depend on the slow space and time coordinates  $\zeta = \epsilon(x - v_g t)$  and  $\tau = \epsilon^2 t$ . Here  $\epsilon$  ( $\ll 1$ ) is a real constant and  $v_g = d\omega/dk$  is the group velocity (depicted in Fig. 1b). Omitting unnecessary details of the method, which may be found elsewhere [25], we shall summarize the relevant results below. The evolution of the leading order ( $\sim \epsilon$ ) electric potential disturbance  $\psi = \phi_1^{(1)}$  is shown to obey a *nonlinear Schrödinger* type evolution equation in the form

$$i \frac{\partial \psi}{\partial \tau} + P \frac{\partial^2 \psi}{\partial \zeta^2} + Q |\psi|^2 \psi = 0, \quad (6)$$

which arises as a compatibility condition at the third order in  $\epsilon$ . Both the dispersion coefficient  $P$  (related to the curvature of the dispersion curve as  $P = \frac{1}{2} \frac{d^2 \omega}{dk^2}$ ), and the nonlinearity coefficient  $Q$  are functions of the wavenumber  $k$  and of the superthermality index  $\kappa$  (in addition to the details of the plasma configuration); the lengthy expressions are omitted here.

According to the established nonlinear modulation theory [25], a wavepacket will be modulationally unstable for  $PQ > 0$ , while on the other hand, it will remain stable for  $PQ < 0$ . Furthermore, in the former case ( $PQ > 0$ ) Eq. (6) possesses a family of *bright-type envelope soliton* solutions, while for  $PQ < 0$  *dark-type* envelope solitons are sustained (see Figs. 5 and 6 below). Remarkably, the ratio  $r = P/Q$  (here depicted in Figure 4, for our model for ion-acoustic wavepackets in kappa-distributed plasmas) determines both the stability profile and the structure of the above solutions. In particular, the threshold for modulational instability to set in is  $\tilde{k}_{cr} = (2Q/P)^{1/2} |\psi_0|$  (here  $\tilde{k}_{cr}$  is the critical wavenumber of an amplitude perturbation and  $|\psi_0|$  is the wavepackets maximum amplitude). On the other hand, the envelope soliton width  $L$  is related to  $\psi_0$  by  $|\psi_0|L = (2P/Q)^{1/2}$ ; therefore, higher/lower values of  $r$  predict a lower/higher instability “window”  $[0, \tilde{k}_{cr}]$  and -independently- wider/narrower envelope excitations, for given maximum amplitude  $|\psi_0|$ .

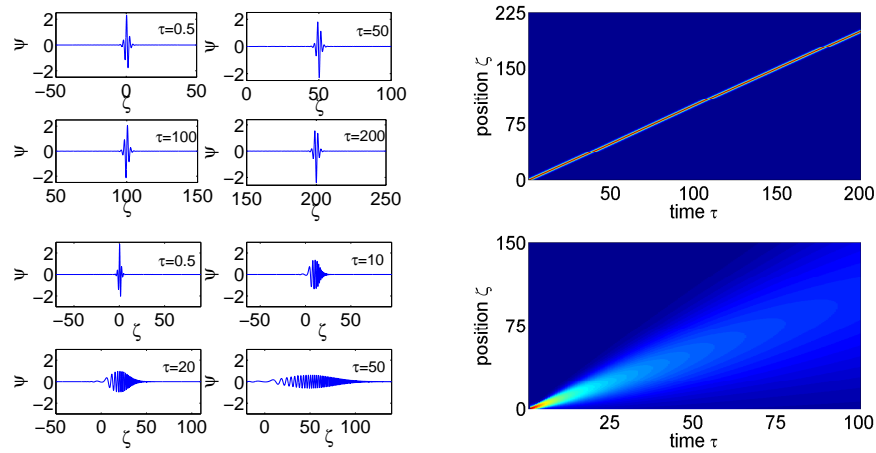


**Figure 5.** (Color online) The evolution of a *bright* envelope soliton is shown for  $k = 1.2$  [20]. The same initial condition (wavepacket) is shown to be (a) stable for  $\kappa = 3$  (since  $PQ > 0$ ) and (b) unstable for  $\kappa = 100$  (since  $PQ < 0$ ), in agreement with the prediction in Fig. 4 [20].

We have tested the stability of a bright-type envelope pulse via numerical integration of Eq. (6). Taking  $k = 1.2$ , Fig. 4 predicts  $r > 0$  for  $\kappa = 3$  but  $r < 0$  for  $\kappa = 100$ . Assuming the same initial condition (in fact, the exact solution soliton for  $\kappa = 3$ ), a *bright-type* envelope (pulse) soliton was shown to propagate in a stable manner in the former (superthermal) case, but then spreads and decays in the latter (Maxwellian) case. These results are depicted in Fig. 5. In an analogous manner, considering the behavior of a *dark-type* envelope (an envelope void) as initial condition for the same plasma conditions, we notice that the wavepacket is stable exactly in the case when its bright sister would be unstable, and vice versa. These results are depicted in Fig. 6.

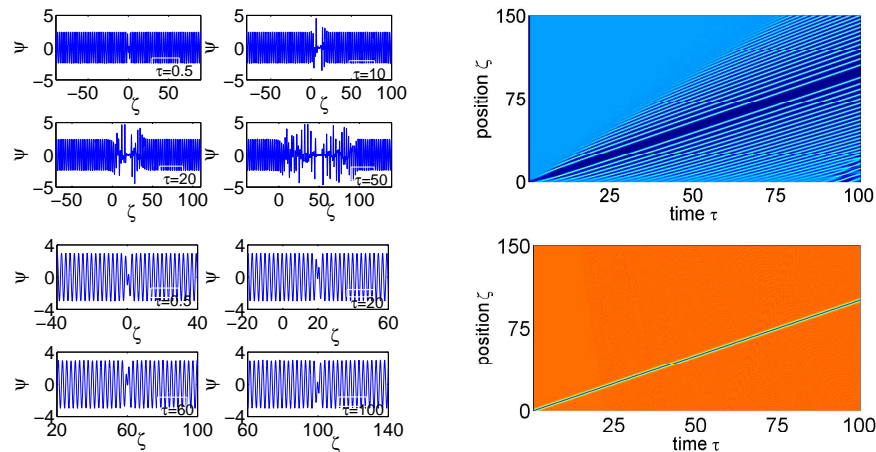


**Figure 6.** (Color online) The evolution of a *dark-type* envelope soliton is shown, for the same values as in the previous Figure ( $k = 1.2$ ). The same initial condition (wavepacket) is shown to be (a) *unstable* for  $\kappa = 3$  (since  $PQ > 0$ ) and (b) *stable* for  $\kappa = 100$  (since  $PQ < 0$ ), in agreement with the prediction in Fig. 4 [20].

As a final remark, the modulational instability growth rate was shown to be strongly modified (and often increased) by considering low values of  $\kappa$ . Excess electron superthermality thus appears to enhance modulational instability of electrostatic wavepackets.

## 5. Summary

We have discussed the fundamental aspects of superthermal particle distributions in space and laboratory plasmas. Focusing on the modeling of nonlinear electrostatic waves propagating in plasmas in the presence of an excess superthermal particle component, we have investigated the basic impact of the latter on the waves' dynamical characteristics and stability profile. We have employed a simple (ion-)fluid model, to discuss the occurrence and dynamics of solitary waves (pulses) as well as envelope solitons. This is a short summary of an extensive series of theoretical investigations, part of which will be reported in forthcoming reports.

A brief comment is in order, for the sake of completeness, on alternative theories proposed for the study of nonthermal plasmas, of which the kappa distribution is but one – albeit most successful – representative. The model proposed by Cairns *et al.* [26] predicts the appearance of bilateral “wings” in the electron distribution, and remarkably accounts for a change in the soliton polarity (e.g., predicts negative potential pulses for ionic dynamics), in agreement with spacecraft observation [26]. Alternative forms of the kappa distribution have also been proposed (see the discussion in [3]). Interestingly, some recent studies [27,28] claim to establish an analogy between the kappa theory and the recently proposed Tsallis theory [29] for non-extensive thermodynamics. Finally, a recently suggested *ad hoc* hybrid-Cairns-Tsallis model [30] seems to combine the pros and cons of both models into a double-parametric phenomenology, which may be an interesting line of research [31].

Concluding, although this admittedly remains a controversial issue, and various fundamental questions need to be addressed, the ubiquity of the kappa distribution, however phenomenologically introduced, appears to have its foundations in an underlying physical truth which is still not elucidated. Our efforts aim at contributing a modest piece of knowledge in this direction, but the largest part of the truth is likely still to be found.

## Acknowledgments

The content of this article was presented as an invited paper at the joint EPS/ICPP 2012 conference (39th EPS Conference on Plasma Physics, 16th International Congress on Plasma Physics) held in Stockholm, Sweden (2-6 July, 2012). The authors acknowledge financial support from UK Engineering and Physical Sciences Research Council (EPSRC) under grants No. EP/I031766/1 (IK) and EPD06337X1 (IK, SS). M.A.H. acknowledges the National Research Foundation of South Africa (NRF) for financial support. Any opinion, findings and conclusions or recommendations expressed in this material are those of the authors and therefore, NRF does not accept any liability in regard thereto. Extensive inspiring discussions with Marco Borghesi, Gianluca Sarri and Vikrant Saxena (Queen's University Belfast, UK), Thomas Baluku (Pwani University College, Kenyatta University, Kenya), Mark Eric Dieckmann (Linköping University, Sweden) and Frank Verheest (Ghent University, Belgium) are warmly



acknowledged. Figures 2 and 3 are reprinted with permission from I. Kourakis and S. Sultana, AIP Conf. Proc. **1397**, 86 (2011) [19] (Copyright 2011, American Institute of Physics).

- [1] V.M. Vasyliunas, J. Geophys. Res. **73**, 2839 (1968).
- [2] V. Pierrard & M. Lazar, Solar Phys. **267**, 153 (2010).
- [3] M.A. Hellberg, R.L. Mace, T.K. Baluku, I. Kourakis and N. S. Saini, Phys. Plasmas **16**, 094701 (2009).
- [4] P. Schippers *et al.*, J. Geophys. Res. **113**, A07208 (2008).
- [5] See, e.g., T.K. Baluku, M. A. Hellberg and R.L. Mace, J. Geophys. Res. **116**, A04227 (2011); T.K. Baluku and M.A. Hellberg, Phys. Plasmas, **19**, 012106 (2012).
- [6] R. Gaelzer *et al.*, J. Geophys. Res. **115**, A09109 (2010).
- [7] M.V. Goldman, D.L. Newman and A. Mangeney, Phys. Rev. Lett., **99**, 145002 (2007), Phys. Rev. Lett. **99**, 145002 (2007); G. Sarri *et al*, Phys. Plasmas **17**, 010701 (2010).
- [8] G. Sarri *et al*, Phys. Plasmas **17**, 082305 (2010).
- [9] G. Sarri, M.E. Dieckmann, I. Kourakis and M. Borghesi, Phys. Rev. Lett. **107**, 025003 (2011)
- [10] D. A. Bryant, J. Plasma. Phys. **56**, 87 (1996); R. Mace, M.A. Hellberg and R.A. Treumann, J. Plasma Phys., **59**, 393 (1998).
- [11] N.S. Saini, I. Kourakis and M.A. Hellberg, Phys. Plasmas **16**, 062903 (2009).
- [12] S. Sultana, I. Kourakis, N.S. Saini and M.A. Hellberg, Phys. Plasmas **17**, 032310 (2010).
- [13] T.K. Baluku, M.A. Hellberg, I. Kourakis and N.S. Saini, Phys. Plasmas **17** 053702 (2010).
- [14] A. Danehkar, N.S. Saini, M.A. Hellberg, and I. Kourakis, Phys. Plasmas **18**, 072902 (2011).
- [15] S. Sultana and I. Kourakis, Plasma Phys. Cont. Fusion **53**, 045003 (2010).
- [16] S. Sultana and I. Kourakis, Eur. Phys. J. D, **66**, 100 (2012)
- [17] S. Sultana, G. Sarri & I. Kourakis, Physics of Plasmas, **19**, 012310 (2012).
- [18] M. Jenab, I. Kourakis, T.K. Baluku and M.A. Hellberg, in preparation.
- [19] I. Kourakis and S. Sultana, AIP Conf. Proc. **1397**, 86 (2011); note that this paper also took into account fixed (immobile) charged dust particulates, an aspect beyond our scope here.
- [20] Presence of a small charged dust component in the plasma is considered in this plot, viz.,  $n_{e0}/n_{i0} = 0.9$ .
- [21] I. Kourakis & P.K. Shukla, Phys. Plasmas **10**, 3459 (2003).
- [22] S. Ghosh, S. Sarkar, M. Khan, and M. R. Gupta, Phys. Plasmas **9**, 378 (2002).
- [23] R.Z. Sagdeev, Rev. Plasma Phys. **4**, 23 (1966).
- [24] A weak dust presence is considered in this plot, viz.,  $n_{e0}/n_{i0} = 0.99$ .
- [25] I. Kourakis and P. K. Shukla, Nonlin. Proc. Geophys., **12**, 407 (2005).
- [26] R.A. Cairns *et al.*, Geophys. Res. Lett. **22**, 2709 (1995).
- [27] A.V. Milovanov and I.M. Zelenyi, Nonlin. Proc. Geophys., **7**, 211 (2000).
- [28] G. Livadiotis and D.J. McComas, J. Geophys. Res. **114**, A011105 (2009).
- [29] C. Tsallis, J. Stat. Phys. **52**, 479 (1988).
- [30] M. Tribeche, R. Amour and P. Shukla, Phys. Rev. E, **85**, 037401 (2012).
- [31] G. Williams, S. Sultana & I. Kourakis, Proc. 39th EPS Conf. on Plasma Physics & 16th Int. Congress Plasma Phys. (ICPP), Stockholm, Sweden (2012), paper P4.097.